Localization Transition for Light Scattering by Cold Atoms in an External Magnetic Field

S. E. Skipetrov*
Université Grenoble Alpes, CNRS, LPMMC, 38000 Grenoble, France

(Received 11 May 2018; published 29 August 2018)

We establish a localization phase diagram for light in a random three-dimensional (3D) ensemble of motionless two-level atoms with a threefold degenerate upper level, in a strong static magnetic field. Localized modes appear in a narrow spectral band when the number density of atoms ρ exceeds a critical value $\rho_c \simeq 0.1k_0^3$, where k_0 is the wave number of light in the free space. A critical exponent of the localization transition taking place upon varying the frequency of light at a constant $\rho > \rho_c$ is estimated to be $\nu = 1.57 \pm 0.07$. This classifies the transition as an Anderson localization transition of 3D orthogonal universality class.

DOI: 10.1103/PhysRevLett.121.093601

The search for Anderson localization of light in three-dimensional (3D) disordered media has been an active research direction since the mid 1980s when John [1] and Anderson [2] independently noticed that light could be localized by strong disorder in a way analogous to electron localization in disordered solids [3]. It was rapidly recognized that optical localization in a dielectric material is difficult to achieve because, on the one hand, of the way in which the disorder enters the optical wave equation [the position-dependent dielectric function $\varepsilon(\mathbf{r})$ of the material multiplies the second-order time derivative of the electric field] and, on the other hand, of the relatively low values of ε of available transparent materials at optical frequencies [4]. Unfortunately, even the materials composed of particles with the largest available dielectric constants did not allow for an indisputable observation of disorder-induced light localization in three dimensions thus far [5–7].

A random spatial arrangement of motionless atoms represents an alternative to dielectric media for reaching Anderson localization of light [8,9]. Indeed, the coherent backscattering (CBS) of light, considered as a precursor of localization, was observed in cold atomic gases almost 20 years ago [10–12]. However, the vector character of light and the associated dipole-dipole interactions between atoms have been predicted to prevent Anderson localization in atomic systems [13,14]. A static external magnetic field partially suppresses the interatomic dipole-dipole interactions and can induce localization of light that is quasiresonant with a $J_g = 0 \to (J_e = 1, m = \pm 1)$ transition (J_g and J_e are the total angular momenta of the atomic ground and excited states, respectively, and m is the magnetic quantum number of the excited state) [15]. It is important to stress that the role played here by the magnetic field is different from that reported in Ref. [12] where the field enhances the CBS contrast for light scattered by a cloud of Rb atoms. In the latter case, the magnetic field lifts the degeneracy of the atomic *ground* state ($J_g > 0$) and thus suppresses Raman scattering and lengthens the coherence length of light. We consider atoms with a nondegenerate ground state ($J_g = 0$) and no Raman scattering. The magnetic field can have only a negative impact on such interference effects as CBS because the contrast of the latter is already maximum in the absence of the field. Therefore, understanding of Anderson localization in our system cannot be achieved with far-field interference arguments and requires dealing with near-field effects, such as the dipole-dipole interactions.

Although the presence of localized modes in the atomic system subjected to an external magnetic field has been already established in Ref. [15], the transition between extended and localized regimes has not been studied yet. This transition takes place in a dense medium that is made strongly anisotropic by the magnetic field, and in the presence of near-field couplings between atoms separated by less than a wavelength in distance. Questions thus arise concerning the nature of this transition: To which extent can it be considered a genuine, disorder-induced Anderson transition? What is its universality class? Does the anisotropy of the atomic medium in a strong magnetic field play any role? It is the purpose of this Letter to provide exhaustive answers to these questions and thereby motivate the experimental work on Anderson localization of light by cold atoms.

An ensemble of N identical two-level atoms (resonance frequency ω_0, $J_g = 0$ for the ground state, $J_e = 1$ for the excited states) at positions $\{\mathbf{r}_j\}$, $j = 1, \ldots, N$, subjected to a constant external magnetic field $\mathbf{B} \| \mathbf{e}_z$ and interacting with a free electromagnetic field, is described by the following Hamiltonian [16–18]:

$$\hat{H} = \sum_{j=1}^{N}\sum_{m=-1}^{1}(\hbar\omega_0 + g_e\mu_B Bm)|e_{jm}\rangle\langle e_{jm}| + \sum_{\boldsymbol{\epsilon}\perp\mathbf{k}}\hbar ck\left(\hat{a}^\dagger_{\mathbf{k}\boldsymbol{\epsilon}}\hat{a}_{\mathbf{k}\boldsymbol{\epsilon}} + \frac{1}{2}\right) - \sum_{j=1}^{N}\hat{\mathbf{D}}_j\cdot\hat{\mathbf{E}}(\mathbf{r}_j) + \frac{1}{2\varepsilon_0}\sum_{j\neq n}^{N}\hat{\mathbf{D}}_j\cdot\hat{\mathbf{D}}_n\delta(\mathbf{r}_j-\mathbf{r}_n). \quad (1)$$

Here we denote the atomic dipole operators by $\hat{\mathbf{D}}_j$, the electric displacement vector by $\varepsilon_0\hat{\mathbf{E}}(\mathbf{r})$, the photon creation and annihilation operators corresponding to a mode of the free electromagnetic field having a wave vector $\mathbf{k}$ and a polarization $\boldsymbol{\epsilon}$ by $\hat{a}^\dagger_{\mathbf{k}\boldsymbol{\epsilon}}$ and $\hat{a}_{\mathbf{k}\boldsymbol{\epsilon}}$, respectively. μ_B is the Bohr magneton, and g_e is the Landé factor of the excited state. As discussed previously [15,19], the quasimodes of the atomic subsystem can be found as eigenvectors of a $3N\times 3N$ effective Hamiltonian G of the open system of atoms interacting via the electromagnetic field:

$$G_{e_{jm}e_{nm'}} = (i-2m\Delta)\delta_{e_{jm}e_{nm'}} - \frac{2}{\hbar\Gamma_0}(1-\delta_{e_{jm}e_{nm'}}) \times \sum_{\mu,\nu} d^\mu_{e_{jm}g_j} d^\nu_{g_n e_{nm'}} \frac{e^{ik_0 r_{jn}}}{r^3_{jn}}\left\{\delta_{\mu\nu}[1-ik_0r_{jn}-(k_0r_{jn})^2] - \frac{r^\mu_{jn}r^\nu_{jn}}{r^2_{jn}}[3-3ik_0r_{jn}-(k_0r_{jn})^2]\right\}, \quad (2)$$

where $k_0=\omega_0/c$, $\Delta = g_e\mu_B B/\hbar\Gamma_0$ is the Zeeman shift in units of the spontaneous decay rate Γ_0, $\mathbf{d}_{e_{jm}g_j} = \langle J_e m|\hat{\mathbf{D}}_j|J_g 0\rangle$, and $\mathbf{r}_{jn}=\mathbf{r}_j-\mathbf{r}_n$. The complex eigenvalues Λ_n of the matrix G yield eigenfrequencies $\omega_n=\omega_0-(\Gamma_0/2)\mathrm{Re}\Lambda_n$ and decay rates $\Gamma_n/2=(\Gamma_0/2)\mathrm{Im}\Lambda_n$ of quasimodes. From here on, we consider atoms that are randomly distributed in a ball of radius R and volume V with an average density $\rho=N/V$.

In a strong magnetic field, the eigenvalues Λ_n split in three groups corresponding to transitions between the ground state and one of the three Zeeman sublevels ($m=0,\pm1$), which now have different frequencies $\omega_m=\omega_0+m\Gamma_0\Delta$ [15]. Each group occupies a roughly circular area of radius $b_0\sim R/\ell_0$ on the complex plane [20,21]. Here $\ell_0\sim k_0^2/\rho$ is the on-resonance scattering mean-free path computed in the independent-scattering approximation (ISA) and b_0 is the on-resonance optical thickness. If the distance between eigenvalue groups on the complex plane 2Δ is much larger than $2b_0$, each group can be found independently by diagonalizing an $N\times N$ matrix $\mathcal{G}^{(m)}$. For $m=\pm1$, we find [21]

$$\mathcal{G}^{(\pm1)}_{jn} = (i\mp 2\Delta)\delta_{jn} + (1-\delta_{jn})\frac{3}{2}\frac{e^{ik_0r_{jn}}}{k_0r_{jn}} \times\left(P(ik_0r_{jn}) + Q(ik_0r_{jn})\frac{\sin^2\theta_{jn}}{2}\right), \quad (3)$$

where $P(x)=1-1/x+1/x^2$ and $Q(x)=-1+3/x-3/x^2$. Note that Eq. (3) still contains divergent near-field terms $\propto 1/r^3_{jn}$ associated with dipole-dipole interactions between atoms, but their magnitude is partially suppressed with respect to the case of $\mathbf{B}=0$ [13]. The effective anisotropy of the atomic medium in a strong magnetic field, which is not obvious from Eq. (2), now becomes evident because Eq. (3) contains an explicit dependence on the angle θ_{jn} between $\mathbf{r}_{jn}$ and $\mathbf{B}$. A comparison of eigenvalues of the matrices (2) and (3) and a discussion of the condition of validity $\Delta\gg b_0$ of Eq. (3) can be found in the Supplemental Material [21].

We will use Eq. (3) to study the localization transition for light that is quasiresonant with the transition between the ground state and one of the excited states corresponding to $m=\pm1$ (there is no localization transition for $m=0$ [15]). To identify the critical points (mobility edges), we use the approach developed in Ref. [28] for scalar waves. In brief, at a fixed (and sufficiently high) density ρ and for a set of different atom numbers N, we compute the eigenvalues Λ_n of the matrix (3) for an ensemble of random atomic configurations $\{\mathbf{r}_j\}$ and then estimate the probability density $p(\ln g;\mathrm{Re}\Lambda,N)$ of the logarithm of the Thouless conductance $g=\mathrm{Im}\Lambda_n/\langle\mathrm{Re}\Lambda_n-\mathrm{Re}\Lambda_{n-1}\rangle$, where the angular brackets denote ensemble averaging. The small-g part of $p(\ln g;\mathrm{Re}\Lambda,N)$ becomes independent of N at the critical points $\mathrm{Re}\Lambda_c$. Instead of working with $p(\ln g;\mathrm{Re}\Lambda,N)$, it is more convenient to analyze its low-rank ($q\leq 0.05$) percentiles $\ln g_q$ defined by $q=\int_{-\infty}^{\ln g_q}p(\ln g;\mathrm{Re}\Lambda,N)d(\ln g)$. Figure 1(a) shows the third percentile ($q=0.03$) as a function of $\mathrm{Re}\Lambda$ for different N. The crossing points of lines corresponding to different N provide approximate positions of mobility edges $\mathrm{Re}\Lambda_c$ shown by vertical dashed lines.

The finite-size scaling analysis of the localization transition consists in fitting the numerical data for $\ln g_q$ near a critical point by polynomials [28,29]:

$$\ln g_q = \sum_{j_1=0}^{n_1}\sum_{j_2=0}^{n_2} a_{j_1j_2}u_1(w)^{j_1}u_2(w)^{j_2}(k_0R)^{j_1/\nu+j_2y}, \quad (4)$$

$$u_i(w) = \sum_{j=0}^{m_i} b_{ij}w^j, \quad (5)$$

where $w=(\mathrm{Re}\Lambda-\mathrm{Re}\Lambda_c)/\mathrm{Re}\Lambda_c$, ν is a critical exponent of the localization transition, and $y<0$ is an irrelevant exponent accounting for deviations from the single-parameter scaling. $m_1=1$, $n_1=2$, $m_2=n_2=1$ in Eqs. (4) and (5) are the minimum values that yield fits of acceptable quality and, at the same time, give consistent values of best-fit $\mathrm{Re}\Lambda_c$ and ν for all q from 0.001 to 0.05. An example of fit is shown in Fig. 1(b) whereas Fig. 2 shows the best-fit values of the mobility edge, corresponding to $\mathrm{Re}\Lambda_c+2m\Delta\simeq-1$ in Fig. 1(a), and of the critical

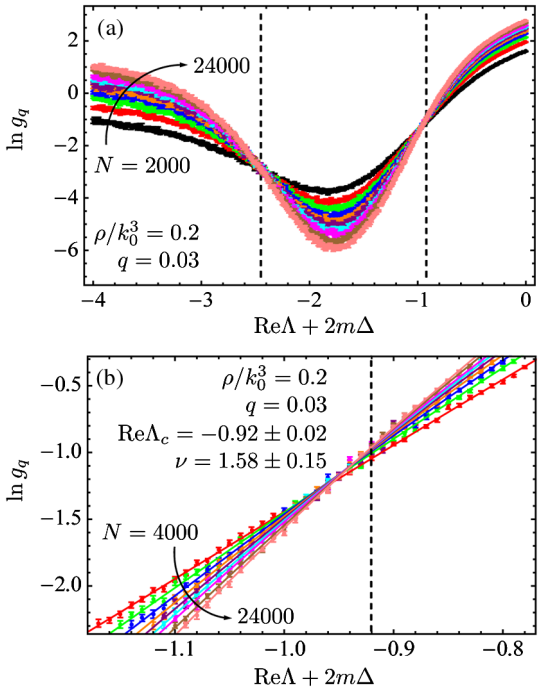

FIG. 1. (a) Third percentile ($q = 0.03$) of the logarithm of Thouless conductance g as a function of frequency at a fixed number density of atoms $\rho/k_0^3 = 0.2$ for 10 different sizes of the atomic cloud: $N = 2000$, 4000, 6000, 8000, 10 000, 12 000, 14 000, 16 000, 20 000, and 24 000 (symbols with error bars). At least 2×10^7 eigenvalues were calculated for each N to compute the percentile. Vertical dashed lines indicate the mobility edges. (b) Fits (solid lines) of Eqs. (4) and (5) to numerical data for $N \geq 4000$ (symbols with error bars) around one of the mobility edges. The best-fit values of the mobility edge $\mathrm{Re}\Lambda_c$ and of the critical exponent ν are given on the graph.

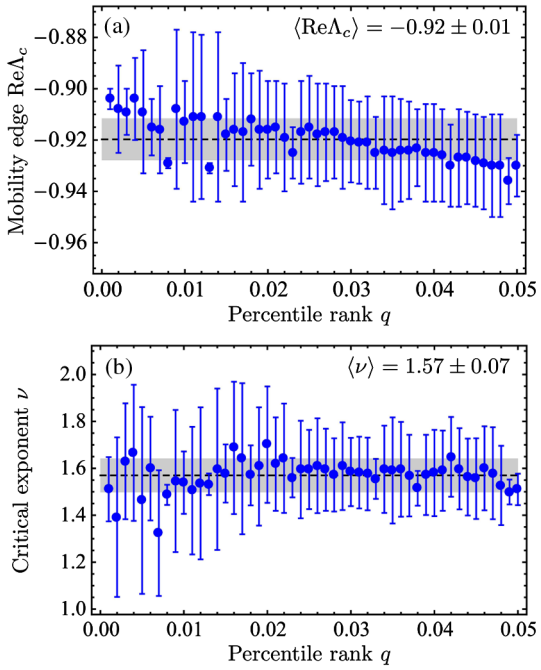

FIG. 2. Best-fit values of the mobility edge $\mathrm{Re}\Lambda_c$ (a) and of the critical exponent ν (b) as functions of the rank q of the analyzed percentile $\ln g_q$. Fits were performed for the data corresponding to $\rho/k_0^3 = 0.2$ and $\ln g_q$ within ± 1 of an estimated crossing point of curves obtained for different N. The dashed solid lines show average values of $\mathrm{Re}\Lambda_c$ and ν, respectively, with the values of the latter printed on the graphs. Gray areas visualize the errors of the averages.

exponent ν as functions of the rank q of the considered percentile for $\rho/k_0^3 = 0.2$. The analysis of the second mobility edge [$\mathrm{Re}\Lambda_c + 2m\Delta \simeq -2.4$ in Fig. 1(a)] is complicated by a stronger noise in the numerical data and does not yield reliable estimations of ν with an acceptable precision.

The best estimate of the critical exponent $\langle\nu\rangle = 1.57 \pm 0.07$ obtained by averaging results obtained for all $q = 0.001$–0.05 [see Fig. 2(b)], is consistent with the value expected for the Anderson transition of the 3D orthogonal universality class, typical for spinless time-reversal (TR) invariant systems [29,30]. The Hamiltonian (1) is formally invariant under TR of the whole system "light + atoms + the magnet creating the magnetic field $\mathbf{B}$" (remember that $\mathbf{B}$ changes sign upon time reversal) [31]. However, for a constant $\mathbf{B}$ that we consider, the subsystem "light + atoms" is not TR invariant and one might expect the localization transition to belong to the unitary universality class and have a different critical exponent [30,32]. To resolve this apparent contradiction, let us consider the transfer of an excitation from an atom n to a distant atom j (see Sec. I of Supplemental Material [21] for details). The transfer is operated by photons of different helicities $\epsilon = \pm 1$ with probability amplitudes $A_{jn}^{(\epsilon)}$. It is not TR invariant because the transfer of an excitation from the atom j back to the atom n by a photon with the same helicity have a different probability amplitude: $A_{nj}^{(\epsilon)} \neq A_{jn}^{(\epsilon)}$. However, this exchange of photons have an additional symmetry imposing $A_{nj}^{(\epsilon)} = A_{jn}^{(-\epsilon)}$. In other words, the photons of positive (negative) helicity play the same role in the excitation transfer from one atom to another as the photons of negative (positive) helicity do for the transfer in the opposite direction. As a result, the exchange of excitations between atoms become TR invariant, and the localization transition in the ensemble of atoms belongs to the orthogonal universality class [33].

The anisotropy induced in the atomic medium by the external magnetic field may play a role in determining the mobility edges [34–36], but apparently does not modify the universality class of the localization transition, in agreement with both previous theoretical results for the anisotropic Anderson model [36] and experiments in cold-atom systems [37].

The analysis performed above for a single atomic density $\rho/k_0^3 = 0.2$ can be repeated for other densities as well. The calculation of ν is very computer-time consuming but

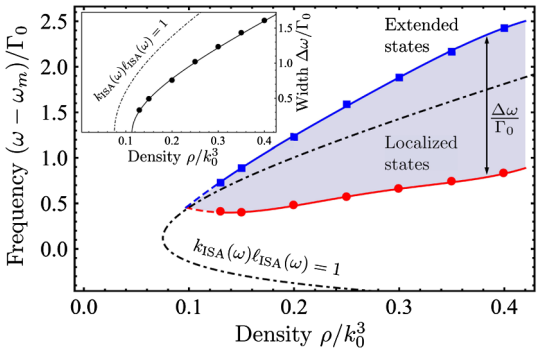

FIG. 3. Localization phase diagram of an ensemble of two-level atoms in a strong magnetic field. The frequency on the vertical axis is measured from $\omega_m = \omega_0 + m\Gamma_0\Delta$ (for $m = \pm 1$) in units of Γ_0. Symbols are mobility edges calculated from at least 10^7 (5.5×10^6) eigenvalues for $N = 8000$ (16 000) at every ρ; lines are polynomial fits. The crossing point of the latter $\rho_c/k_0^3 \simeq 0.1$ is an estimation of the absolute localization threshold. Inset: the width of the frequency band of localized states (circles) fitted by Eq. (6) (solid line) with $\rho_c/k_0^3 \simeq 0.11$ and $\rho^*/k_0^3 \simeq 0.51$. The dash-dotted lines in both the main plot and the inset are obtained from the IR criterion in the ISA [21].

the mobility edges can be estimated from the results for a smaller number of random configurations $\{\mathbf{r}_j\}$ and only two different N, see Fig. 3. For $0.1 \lesssim \rho/k_0^3 \lesssim 0.12$ the mobility edges are too close to be clearly distinguishable, and they disappear for $\rho/k_0^3 < \rho_c/k_0^3 \simeq 0.1$ The latter value also follows from polynomial fits in Fig. 3 as a minimum density at which localized states appear. It is slightly larger than $\rho_c/k_0^3 \simeq 0.08$ identified as the absolute localization threshold for scalar waves [38]. In our opinion, this difference reflects the residual dipole-dipole interactions which are partially suppressed but not fully eliminated by the magnetic field. As a consequence, Anderson localization requires a higher scatterer density and thus is more difficult to reach for light scattered by atoms in a magnetic field than for scalar waves. In addition to this, the region of localized states in the phase diagram of Fig. 3 is significantly shifted upwards with respect to its counterpart for scalar waves [38], its shape is modified and its width is reduced.

Some features of Fig. 3 can be qualitatively understood based on the Ioffe-Regel (IR) criterion of Anderson localization $k\ell = 1$ evaluated in the ISA. Calculating the effective wave number $k(\omega)$ and the scattering mean free path $\ell(\omega)$ in the scalar approximation and in the lowest order in density ρ for an atomic resonance at $\omega = \omega_m$, we obtain the dashed-dotted lines in Fig. 3 [21]. The ISA yields a correct order of magnitude for the minimum density ρ_c needed to reach localization and rightly predicts that the band of localized states is blueshifted with respect to ω_m, although it largely underestimates the magnitude of the shift. The most obvious failure of the ISA in Fig. 3 is its complete incapacity to describe the low-frequency mobility edge. As a consequence, also the width $\Delta\omega$ of the spectral band in which Anderson localization takes place is overestimated. The ISA yields a compact expression for it [21]:

$$\frac{\Delta\omega}{\Gamma_0} = \frac{\pi}{k_0^3}\sqrt{(\rho-\rho_c)(\rho+\rho^*)}, \tag{6}$$

where $\rho_c = k_0^3(\sqrt{5}-2)/\pi$ and $\rho^* = k_0^3(\sqrt{5}+2)/\pi$. This equation is shown in the inset of Fig. 3 by a dash-dotted line. Although Eq. (6) does not describe our numerical results shown by symbols, it can provide a good fit to them if we treat ρ_c and ρ^* as free fit parameters (solid line in the inset of Fig. 3).

It is important to keep in mind that in this work we take two limits in a well-defined order: first $B \to \infty$ and then $N \to \infty$, ensuring that the condition $\Delta \gg b_0$ needed to justify Eq. (3) is always obeyed. Changing the order of limits would require working with the full $3N \times 3N$ matrix G and might modify the results. In an experiment with cold atoms, it should be possible to achieve sufficiently strong fields B to decouple transitions with different magnetic quantum numbers m for a given N (see Ref. [19] for a discussion of a possible experiment). The optical localization transition can be studied by observing the time-dependent fluorescence of a dense atomic system after an excitation by a pulse [19]. The fluorescence is expected to slow down when the frequency and the polarization of the exciting pulse correspond to those of localized quasimodes. Spectral analysis of the signal should allow for identification of frequencies ω_n and decay rates Γ_n of quasimodes as it has been already done in quasi-1D microwave experiments [39], allowing for calculation of Thouless conductance $g(\omega)$ for each atomic configuration. Using "artificial atoms" (quantum dots) may have an advantage of obviating the Doppler and recoil effects inherent for atomic systems [16].

In conclusion, we established the localization phase diagram for light propagating in a dense random 3D ensemble of two-level atoms subjected to a strong magnetic field, and estimated the critical exponent ν of the localization transition taking place upon varying its frequency. The value $\nu = 1.57 \pm 0.07$ obtained from a finite-size scaling analysis, indicates that the transition is an Anderson transition of 3D orthogonal universality class, despite the broken time-reversal symmetry of the system "light + atoms" which might have changed its universality class into the unitary one, but is compensated by a symmetry between photons of opposite helicities propagating in opposite directions. The transition frequencies are blueshifted with respect to the atomic resonances $\omega_0 \pm \Gamma_0\Delta$ and the minimum number density of atoms required to reach the transition is $\rho_c \simeq 0.1k_0^3$. These features of the phase diagram are qualitatively reproduced by the IR criterion of localization evaluated in the ISA. However, the latter criterion fails to provide quantitatively accurate results. The anisotropy induced in the atomic medium by

the external magnetic field does not modify the universality class of the localization transition.

This work was funded by the Agence Nationale de la Recherche (Grant No. ANR-14-CE26-0032 LOVE). All the computations presented in this Letter were performed using the Froggy platform of the CIMENT infrastructure, which is supported by the Rhone-Alpes region (Grant No. CPER07_13 CIRA) and the Equip@Meso project (reference ANR-10-EQPX-29-01) of the programme Investissements d'Avenir supervised by the Agence Nationale de la Recherche.

*sergey.skipetrov@lpmmc.cnrs.fr

[1] S. John, Electromagnetic Absorption in a Disordered Medium Near a Photon Mobility Edge, Phys. Rev. Lett. **53**, 2169 (1984).
[2] P. W. Anderson, The question of classical localization: A theory of white paint? Philos. Mag. B **52**, 505 (1985).
[3] P. W. Anderson, Absence of diffusion in certain random lattices, Phys. Rev. **109**, 1492 (1958).
[4] S. John, Localization of light, Phys. Today **44**, 32 (1991).
[5] T. van der Beek, P. Barthelemy, P. M. Johnson, D. S. Wiersma, and A. Lagendijk, Light transport through disordered layers of dense gallium arsenide submicron particles, Phys. Rev. B **85**, 115401 (2012).
[6] T. Sperling, L. Schertel, M. Ackermann, G. J. Aubry, C. M. Aegerter, and G. Maret, Can 3D light localization be reached in 'white paint'?, New J. Phys. **18**, 013039 (2016).
[7] S. E. Skipetrov and J. H. Page, Red light for Anderson localization, New J. Phys. **18**, 021001 (2016).
[8] R. Kaiser, Cold atoms and multiple scattering, in *Diffuse Waves in Complex Media*, ed. by J.-P. Fouque (Kluwer, Dordrecht, 1999), p. 249.
[9] R. Kaiser, Quantum multiple scattering, J. Mod. Opt. **56**, 2082 (2009).
[10] G. Labeyrie, F. de Tomasi, J.-C. Bernard, C. A. Müller, C. Miniatura, and R. Kaiser, Coherent Backscattering of Light by Cold Atoms, Phys. Rev. Lett. **83**, 5266 (1999).
[11] Y. Bidel, B. Klappauf, J. C. Bernard, D. Delande, G. Labeyrie, C. Miniatura, D. Wilkowski, and R. Kaiser, Coherent Light Transport in a Cold Strontium Cloud, Phys. Rev. Lett. **88**, 203902 (2002).
[12] O. Sigwarth, G. Labeyrie, T. Jonckheere, D. Delande, R. Kaiser, and C. Miniatura, Magnetic Field Enhanced Coherence Length in Cold Atomic Gases, Phys. Rev. Lett. **93**, 143906 (2004).
[13] S. E. Skipetrov and I. M. Sokolov, Absence of Anderson Localization of Light in a Random Ensemble of Point Scatterers, Phys. Rev. Lett. **112**, 023905 (2014).
[14] L. Bellando, A. Gero, E. Akkermans, and R. Kaiser, Cooperative effects and disorder: A scaling analysis of the spectrum of the effective atomic Hamiltonian, Phys. Rev. A **90**, 063822 (2014).
[15] S. E. Skipetrov and I. M. Sokolov, Magnetic-Field-Driven Localization of Light in a Cold-Atom Gas, Phys. Rev. Lett. **114**, 053902 (2015).
[16] C. Cohen-Tannoudji, J. Dupont-Roc, and G. Grynberg, *Photons and Atoms: Introduction to Quantum Electrodynamics* (Wiley, New York, 1992).
[17] O. Morice, Y. Castin, and J. Dalibard, Refractive index of a dilute Bose gas, Phys. Rev. A **51**, 3896 (1995).
[18] O. Sigwarth, G. Labeyrie, D. Delande, and C. Miniatura, Multiple scattering of light in cold atomic clouds in a magnetic field, Phys. Rev. A **88**, 033827 (2013).
[19] S. E. Skipetrov, I. M. Sokolov, and M. D. Havey, Control of light trapping in a large atomic system by a static magnetic field, Phys. Rev. A **94**, 013825 (2016).
[20] S. E. Skipetrov and A. Goetschy, Eigenvalue distributions of large Euclidean random matrices for waves in random media, J. Phys. A **44**, 065102 (2011).
[21] See Supplemental Material at http://link.aps.org/supplemental/10.1103/PhysRevLett.121.093601 for a derivation and a study of validity of the scalar model (3), and a derivation of the localization phase diagram from the IR criterion. The Supplemental Material includes Refs. [22–27].
[22] A. F. Ioffe and A. R. Regel, Non-crystalline, amorphous and liquid electronic semiconductors, in *Progress in Semiconductors*, edited by A. F. Gibson (Wiley, New York, 1960), Vol. 4, p. 237.
[23] P. Sheng, *Introduction to Wave Scattering, Localization and Mesoscopic Phenomena* (Academic Press, San Diego, 1995).
[24] A. Lagendijk and B. A. van Tiggelen, Resonant multiple scattering of light, Phys. Rep. **270**, 143 (1996).
[25] P. de Vries, D. V. van Coevorden, and A. Lagendijk, Point scatterers for classical waves, Rev. Mod. Phys. **70**, 447 (1998).
[26] J. Javanainen, J. Ruostekoski, Y. Li, and S.-M. Yoo, Shifts of a Resonance Line in a Dense Atomic Sample, Phys. Rev. Lett. **112**, 113603 (2014).
[27] S. D. Jenkins, J. Ruostekoski, J. Javanainen, R. Bourgain, S. Jennewein, Y. R. P. Sortais, and A. Browaeys, Optical Resonance Shifts in the Fluorescence of Thermal and Cold Atomic Gases, Phys. Rev. Lett. **116**, 183601 (2016).
[28] S. E. Skipetrov, Finite-size scaling analysis of localization transition for scalar waves in a three-dimensional ensemble of resonant point scatterers, Phys. Rev. B **94**, 064202 (2016).
[29] K. Slevin and T. Ohtsuki, Critical exponent for the Anderson transition in the three-dimensional orthogonal universality class, New J. Phys. **16**, 015012 (2014).
[30] F. Evers and A. D. Mirlin, Anderson transitions, Rev. Mod. Phys. **80**, 1355 (2008).
[31] B. A. van Tiggelen and R. Maynard, Reciprocity and coherent backscattering of light, in *Wave Propagation in Complex Media. The IMA Volumes in Mathematics and its Applications*, ed. by G. Papanicolaou (Springer, New York, NY, 1998), Vol. 96, p. 247.
[32] K. Slevin and T. Ohtsuki, The Anderson Transition: Time Reversal Symmetry and Universality, Phys. Rev. Lett. **78**, 4083 (1997).
[33] Note that the effective Hamiltonian (3) is non-Hermitian and hence is formally not invariant under TR: $\mathcal{G}_{jn}^{(\pm 1)} \neq \mathcal{G}_{nj}^{(\pm 1)*}$. This breakdown of TR is due to the openness of the considered system and should not be taken into account when discussing the universality class of the localization transition which, by definition, takes place in the *infinite* medium.

[34] A. A. Abrikosov, Anderson localization in strongly anisotropic metals, Phys. Rev. B **50**, 1415 (1994).
[35] B. C. Kaas, B. A. van Tiggelen, and A. Lagendijk, Anisotropy and Interference in Wave Transport: An Analytic Theory, Phys. Rev. Lett. **100**, 123902 (2008).
[36] F. Milde, R. A. Römer, M. Schreiber, and V. Uski, Critical properties of the metal-insulator transition in anisotropic systems, Eur. Phys. J. B **15**, 685 (2000).
[37] M. Lopez, J.-F. Clément, P. Szriftgiser, J. C. Garreau, and D. Delande, Experimental Test of Universality of the Anderson Transition, Phys. Rev. Lett. **108**, 095701 (2012).
[38] S. E. Skipetrov and I. M. Sokolov, Ioffe-Regel criterion of Anderson localization in the model of resonant point scatterers, arXiv:1803.11479 [Phys Rev. B (to be published)].
[39] J. Wang and A. Z. Genack, Transport through modes in random media, Nature (London) **471**, 345 (2011).